Cooperative Control of Energy Storage for Transient Stability Enhancement

Rodrigo D. Trevizan, Muharrem Ayar and Arturo S. Bretas
Dept. Electrical and Computer Eng.
University of Florida
Gainesville, Florida
rodtrevizan@ufl.edu, muharremx@ufl.edu, arturo@ece.ufl.edu

Serhat Obuz
Dept. Electrical and Electronics Eng.
Eskisehir Osmangazi University
Eskisehir, Turkey
sobuz@ogu.edu.tr

***Abstract*—The increasing adoption of inertia-less power sources raises concerns with respect to the ability of the power grid of the future in resisting large disturbances. In this paper, we propose a method that leverages fast-acting energy storage to stabilize generators when subject to contingencies. This is done by a cooperative control protocol capable of coordinating the control actions of neighboring control agents. The goals of this controller is achieving rotor speed synchronism between nearby generators and limiting the rotor angular frequency deviation from nominal values. The distributed protocol is tested using IEEE 39-bus test system implemented in MATLAB/Simulink. The results show that the designed controller can increase the critical clearing time of the system when compared to classical power system stabilizers and a parametric feedback linearization method that leverages energy storage systems.**

***Index Terms*—Cooperative control, distributed control, distributed energy storage, power system stability, transient stability.**

I. Introduction

The increasing presence of renewable sources of electric energy connected to the power grid is disrupting the current paradigm of power systems. Not only it represents a change in the relations between utilities, ISOs, electricity producers and consumers, but also it is speeding up the need for grid modernization. A significant amount of newly installed power generation sources is power-electronics interfaced. The flexibility of inverters is yet to be fully harnessed, but its shortcomings can be already felt. Transient stability, which is the ability of a power system to resist large disturbances, hugely relies on the inertia of synchronous generators. However, the increasing deployment of low-inertia power generation, especially from solar and wind power, is displacing classical high-inertia generators, such as nuclear, coal and gas power plants, thus raising concerns with respect to the stability of smart grids. The reduction of inertia harms the ability of the grid to withstand large contingencies, such as the loss of a large generator or an abrupt load change. Given this reduction in transient stability margins, the next generation of smart grid technology must enhance its stabilizing mechanisms.

One candidate solution, Distributed Energy Storage Systems (DESS), such as flywheels and grid-connected batteries, are currently being deployed to perform frequency regulation and load following [1], but their potential for grid stabilization remains unused. Failing to stabilize a generator triggers protection equipment that disconnects it from the grid. The loss of a generating unit has a huge effect on the load flows of the power grid that can overload power lines, then triggering complex cascading failures [2].

We consider three different control paradigms for large and distributed dynamical systems: centralized, distributed and decentralized [3]. Centralized schemes use the knowledge of all system states to actuate, while decentralized schemes only require local measurements to function. Distributed (or cooperative) schemes are a hybrid of the former and latter, requiring information from both local and neighboring states, thus partial system knowledge. With respect to the stability of the smart grid, one can say that distributed controllers are more robust to physical and communication failures than their centralized counterparts [3]. Additionally, centralized architectures inherently have single point of failure and they also might be susceptible to failure under islanding, when the power system is split into two or more disconnected components. Distributed control's performance is limited because it only uses limited information from local and neighboring sources, however its efficiency can be improved by coordinating between agents. An example of a very robust distributed system is the internet. In [4], a decentralized Feedback Linearization Control (FBLC) is introduced as an improvement over classical linear constant-gain PSS controllers. In [5] a Parametric Feedback Linearization (PFL) is introduced for stabilization of the smart grid. It is considered that generator units are equipped with PMUs, a controller with access to PMU data from neighboring generators and a fast-acting DESS actuated by a parametric FBLC controller. One limitation of this solution is the requirement of the precise knowledge of the nonlinear component to be canceled demanded by the FBLC. Previously, the authors have developed robust controllers with time-delay compensation considering decentralized [6] and distributed paradigms [7] for transient stability enhancement, also resilient to cyber-attacks and errors in measurements [8].

While transient stability depends on maintaining synchronism between synchronous machines [9], these techniques focus on local or neighboring information, such as local rotor speed and local or neighboring voltage angles, which are a very limited measure of synchronism of a generator

with respect to other machines in the system. Moreover, the dynamic models considered in previous works [5]–[8] assume that the power injected by a DESS in a generator node is completely absorbed by the local machine, thus including this term in the swing equation directly.

In this paper, we propose to approach the problem of transient stability with a focus on maintaining synchronism between neighboring synchronous machines. We do so by proposing a consensus-based controller to increase the transient stability margins of smart grids. This multi-agent control protocol coordinates the actions between agents by leveraging the rotor speeds of local and neighboring machines to actuate a DESS connected to the local generator. Another advantage of this paper with respect to previously developed works [5]–[8] is that the proposed control scheme does not require measurements of rotor angles, which are hard to estimate [10]. The main contributions of this paper are twofold:

1) present improved mathematical models that describe the dynamics of the power grid when DESS are connected to the generator buses and
2) propose a novel consensus-based distributed control protocol for the actuation of DESS.

This paper is organized as follows. Section II introduces the architecture of the power grid and its mathematical model. In Section III, the proposed consensus protocol is presented. We present numerical results in Section IV, respectively. Finally, the conclusions of this work are presented in Section V.

II. Architecture of the Distributed Controller

The phenomenon of transient stability is studied during the first few swings. For the sake of simplicity, we consider the simplified second-order differential equation (1) [4] to describe the electromechanical oscillations of a synchronous generator.

$$\begin{aligned} \dot{\delta}_i &= \Delta\omega_i \\ M_i \cdot \dot{\Delta\omega}_i &= -D_i\Delta\omega_i + P_{m,i} - P_{e,i} \end{aligned} \tag{1}$$

where δ_i is the rotor angle, $\Delta\omega_i$ is the deviation of rotor angular frequency from its nominal value, M_i is the machine inertia constant, D_i is a damping constant, $P_{m,i}$ is the mechanical power input from the prime mover and $P_{e,i}$ is the electrical output power of the i-th generator. We consider that each generator has a fast-acting DESS connected to it, as shown in Fig. 1. This figure also shows the differences between terminal voltage magnitudes and angles, $|V^b|$ and δ^b respectively, and the machine internal counterparts, $|V|$ and δ, which are the ones we consider during transient stability studies. Previous works [5]–[8] model the effect of the power injection from the DESS, $P_{s,i}$ by adding this term directly to the the swing equation (1). This model, however, implicitly considers that all the power injected by the DESS is absorbed by the synchronous machine, which is an approximation. An example is shown in Fig. 2, which illustrates the absolute values of susceptances of the Kron-reduced model of IEEE 39-bus system. This reduction is performed by linearizing all

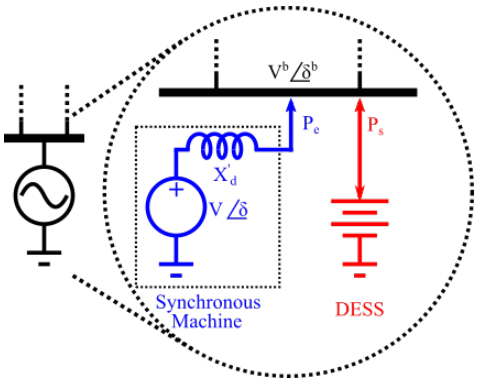

Fig. 1. Structure of each agent showing DESS and synchronous generator connected to the same bus.

loads and reducing the bus admittance matrix from a 39-by-39 (number of buses) to a reduced 10-by-10 model. The resulting reduced susceptance matrix is shown in Fig. 2.

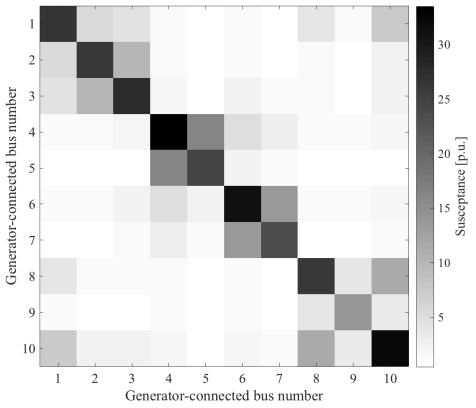

Fig. 2. Per unit absolute values of the susceptance taken from the Kron-reduced admittance bus of the IEEE 39-bus test system showing the electric coupling between generator-connected buses.

The dark spots in Fig. 2 indicate high susceptance between generator terminals. We can identify in this example that strong electrical couplings between neighboring agents do exist and they should be considered in a stabilizing scheme, which will be shown in II-A.

A. Mathematical Description of the Grid Considering DESS

The power exchanges between each agent and other agents and loads are modeled by power flow equations. The power injected to the i-th bus of a power grid can be calculated as:

$$\begin{aligned} P_i = |V_i^b|^2 G_{i,i} + \\ |V_i^b| \sum_{j \in N_i} |V_j^b| \left(G_{i,j} \cos(\delta_i^b - \delta_j^b) + B_{i,j} \sin(\delta_i^b - \delta_j^b) \right) \end{aligned} \tag{2}$$

where P_i is the power injected by the i-th bus, δ_i^b is the generator-connected bus‘ voltage angle and its voltage magnitude is defined as $|V_i^b|$. N_i is the set of all buses connected to the i-th bus (excluding i), $G_{i,j}$ and $B_{i,j}$ are the conductance and susceptance, respectively, between buses i and j. We consider the case where we have performed a Kron reduction of the power grid, therefore the number of buses is equal to

the number of generators and the matrices $\mathbf{G}$ and $\mathbf{B}$ represent respectively the equivalent conductance and susceptance between buses. Furthermore, we can alternatively calculate P_i from $P_{s,i}$ and $P_{e,i}$ by applying Kirchhoff's current law to the i-th node, i.e. $P_i = P_{e,i}+P_{s,i}$, as shown in fig. 1. To model the relation between the machine internal voltage angles, δ_i and the machine terminal, or equivalently generator bus-connected, voltage angles, δ_i^b, we consider a simple transient model for the generator [9]. If we neglect the resistance of the generator and assume it has a round rotor, we can describe $P_{e,i}$ as (3).

$$P_{e,i} = |V_i||V_i^b| \sin(\delta_i - \delta_i^b) X'^{-1}_{d,i} \tag{3}$$

where $X'_{d,i}$ is the transient direct axis reactance of the machine and $|V_i|$ is its equivalent internal voltage.

Now we want to obtain a compact representation for all generators. For a system with Nm generators, we define the vector of rotor angles as $\delta = [\delta_1, \delta_2, ..., \delta_{Nm}]^T$, the vector of bus voltage angles as $\delta^{\mathbf{b}} = [\delta_1^b, \delta_2^b, ..., \delta_{Nm}^b]^T$, rotor angular speeds as $\mathbf{\Delta}\omega = [\Delta\omega_1, \Delta\omega_2, ..., \Delta\omega_{Nm}]^T$, mechanical power as $\mathbf{P_m} = [P_{m,1}, P_{m,2}, ..., P_{m,Nm}]^T$, bus power injection as $\mathbf{P} = [P_1, P_2, ..., P_{Nm}]^T$, the power output of the synchronous machines as $\mathbf{P_e} = [P_{e,1}, P_{e,2}, ..., P_{e,Nm}]^T$, DESS power injection as $\mathbf{P_s} = [P_{s,1}, P_{s,2}, ..., P_{s,Nm}]^T$ and the matrices for machine inertia constants as $\mathbf{M} = diag\{M_1, M_2, ..., M_{Nm}\}$, and damping constants as $\mathbf{D} = diag\{D_1, D_2, ..., D_{Nm}\}$. We can then obtain the dynamic model for the entire grid as:

$$\begin{aligned} \dot{\delta} &= \mathbf{\Delta}\omega \\ \dot{\mathbf{\Delta}\omega} &= \mathbf{M}^{-1}\left(-\mathbf{D}\mathbf{\Delta}\omega + \mathbf{P_m} - \mathbf{P_e}\right) \end{aligned} \tag{4}$$

To simplify the analysis, it is possible to linearize (4) considering constant voltages $|\mathbf{V^b}|$ and $|\mathbf{V}|$. The equations of the dynamic system are linearized at an initial steady-state point of operation given by $\delta^{\mathbf{b,0}}$ and $\delta^{\mathbf{0}}$.

$$\mathbf{\Delta}\delta^{\mathbf{b}} = \delta^{\mathbf{b}} - \delta^{\mathbf{b,0}}, \mathbf{\Delta}\delta = \delta - \delta^{\mathbf{0}} \tag{5}$$

It is also possible to linearize $\mathbf{P}$, $\mathbf{P_e}$ and $\mathbf{P_s}$ as follows:

$$\tilde{\mathbf{P}} = \mathbf{P^0} + \nabla_{\delta^{\mathbf{b}}}\mathbf{P}\mathbf{\Delta}\delta^{\mathbf{b}} \tag{6}$$

$$\tilde{\mathbf{P_e}} = \mathbf{P_e^0} + \nabla_{\delta}\mathbf{P_e}\mathbf{\Delta}\delta + \nabla_{\delta^{\mathbf{b}}}\mathbf{P_e}\mathbf{\Delta}\delta^{\mathbf{b}} \tag{7}$$

$$\mathbf{P_s} = \mathbf{P_s^0} + \mathbf{\Delta P_s} \tag{8}$$

where $\nabla_{\delta}\mathbf{P_e} = [\frac{d}{d\delta_1}\mathbf{P_e}\ \frac{d}{d\delta_2}\mathbf{P_e} \cdots \frac{d}{d\delta_{Nm}}\mathbf{P_e}]$ is the Nm-by-Nm Jacobian matrix of $\mathbf{P_e}$ for derivatives with respect to the angles δ, and similarly $\nabla_{\delta^{\mathbf{b}}}\mathbf{P_e}$ is the Jacobian matrix of $\mathbf{P_e}$ for derivatives with respect to the angles $\delta^{\mathbf{b}}$ and $\nabla_{\delta^{\mathbf{b}}}\mathbf{P}$ is the Jacobian matrix of $\mathbf{P}$ for derivatives with respect to the angles $\delta^{\mathbf{b}}$, all calculated at the operation point. Given that in steady state $\mathbf{P_e^0} = \mathbf{P^0} - \mathbf{P_s^0}$, we can solve for $\mathbf{\Delta}\delta^{\mathbf{b}}$.

$$\mathbf{\Delta}\delta^{\mathbf{b}} = -\left(\nabla_{\delta^{\mathbf{b}}}\mathbf{P_e} - \nabla_{\delta^{\mathbf{b}}}\mathbf{P}\right)^{-1}\left(\nabla_{\delta}\mathbf{P_e}\mathbf{\Delta}\delta + \mathbf{\Delta P_s}\right) \tag{9}$$

Additionally, if (9) is replaced into (7), we can obtain (10).

$$\begin{aligned} \tilde{\mathbf{P_e}} =& \mathbf{P_e^0} + \nabla_{\delta}\mathbf{P_e}\mathbf{\Delta}\delta - \\ & \nabla_{\delta^{\mathbf{b}}}\mathbf{P_e}\left(\nabla_{\delta^{\mathbf{b}}}\mathbf{P_e} - \nabla_{\delta^{\mathbf{b}}}\mathbf{P}\right)^{-1}\left(\nabla_{\delta}\mathbf{P_e}\mathbf{\Delta}\delta + \mathbf{\Delta P_s}\right) \end{aligned} \tag{10}$$

Assuming that the dynamics of the prime mover are slow, we can consider $\mathbf{P_m}$ constant and $\mathbf{P_m} = \mathbf{P_e^0}$. Then we have (11).

$$\begin{aligned} \dot{\mathbf{\Delta}}\delta &= \mathbf{\Delta}\omega \\ \dot{\mathbf{\Delta}}\omega &= \mathbf{M}^{-1}\left(-\mathbf{D}\mathbf{\Delta}\omega - \mathbf{K_{\Delta\delta}}\mathbf{\Delta}\delta + \mathbf{K_{P_s}}\mathbf{\Delta P_s}\right) \end{aligned} \tag{11}$$

where $\mathbf{K_{\Delta\delta}} = \nabla_{\delta}\mathbf{P_e} - \nabla_{\delta^{\mathbf{b}}}\mathbf{P_e}\left(\nabla_{\delta^{\mathbf{b}}}\mathbf{P_e} - \nabla_{\delta_{\mathbf{b}}}\mathbf{P}\right)^{-1}\nabla_{\delta}\mathbf{P_e}$ and $\mathbf{K_{P_s}} = \nabla_{\delta^{\mathbf{b}}}\mathbf{P_e}\left(\nabla_{\delta^{\mathbf{b}}}\mathbf{P_e} - \nabla_{\delta^{\mathbf{b}}}\mathbf{P}\right)^{-1}$. We can rewrite (11) as:

$$\dot{\mathbf{x}} = \mathbf{A_o}\mathbf{x} + \mathbf{B_o}\mathbf{u} \tag{12}$$

where $\mathbf{x} = [\mathbf{\Delta}\delta^T, \mathbf{\Delta}\omega^T]^T$ and $\mathbf{u} = [\mathbf{0}^T, \mathbf{\Delta P_s}^T]^T$ with matrices $\mathbf{A_o}$ and $\mathbf{B_o}$ given by (13).

$$\mathbf{A_o} = \begin{bmatrix} \mathbf{0} & \mathbf{I} \\ -\mathbf{M}^{-1}\mathbf{K_{\Delta\delta}} & -\mathbf{M}^{-1}\mathbf{D} \end{bmatrix}, \mathbf{B_o} = \begin{bmatrix} \mathbf{0} \\ \mathbf{M}^{-1}\mathbf{K_{P_s}} \end{bmatrix} \tag{13}$$

where $\mathbf{0}$ is a Nm-by-Nm matrix of zeros and $\mathbf{I}$ is a Nm-by-Nm identity matrix.

III. Cooperative Control Protocol

In this paper, we support that the stabilization of the power grid after a large disturbance must focus on maintaining synchronism between generators. Therefore we propose a cooperative control strategy to stabilize the system. Distributed control is capable of a higher level of system-wide awareness than decentralized control schemes and lower communication requirements than centralized controllers. This control protocol is designed with two objectives in mind:

1) Maintain synchronism between neighboring agents,
2) Minimize the rotor speed deviation.

The first goal is due to the nature of the problem of transient stability, that is related to synchronism of synchronous generators. The second goal has to do with the fact that achieving synchronism is not enough because generators are required to operate with rotor speed close to the nominal values. If a generator experiences large rotor angle frequency deviations, protection functions such as overspeed, overfrequency and underfrequency might actuate, thus causing an undesirable disconnection of the unit from the grid [11]. Given the linear representation of the system (11) we can now design a cooperative protocol to stabilize the power grid. First we define the local, $e_{l,i}$ and neighboring, $e_{d,i}$ error signals as:

$$e_{l,i} = \Delta\omega_i, e_{d,i} = \sum_{j\in\mathcal{N}_i}\left(\Delta\omega_i - \Delta\omega_j\right) \tag{14}$$

where $\mathcal{N}_i$ is the set of agents that are neighbors of the i-th generator, i.e., synchronous machines that transmit their rotor speed deviation to DESS controller i. The control protocol should be capable of minimizing the differences between rotor angular frequencies of nearby generators (goal 1), which are represented by $e_{d,i}$, and the deviation of the each rotor speed from nominal (goal 2), defined by $e_{l,i}$. Therefore, we propose a simple proportional-integral (PI) controller to minimize both errors and achieve zero-error in steady-state. The control protocol is defined as (15).

$$u_i = -(k_p e_{l,i} + k_{cp} e_{d,i} + \int_0^t \left[k_i e_{l,i}(\tau) + k_{ci} e_{d,i}(\tau)\right] d\tau) \tag{15}$$

where u_i is the i-th control signal, k_p, k_i, k_{cp} and k_{ci} are positive control gains. For simplicity, we consider that all controllers have the same gains. We assume that the dynamics of DESS are very fast, so power is available instantly when required by the controller, i.e., $P_{s,i} = u_i$. Another design requirement of the protocol is defining the topology of the communications network. The communication links between agents are represented by the Nm-by-Nm adjacency matrix $\mathbf{A_d}$, where nonzero $a_{i,j}$ elements represent that there is link that transmits information from node i to node j. In this paper, all the communication links are two-way, therefore $\mathbf{A_d}$ is symmetric. $\mathbf{D_g}$ is the corresponding degree matrix, which is a diagonal matrix whose main-diagonal elements are the sum of the corresponding rows of $\mathbf{A_d}$, and $\mathbf{L}$ is the Laplacian matrix, obtained by $\mathbf{L} = \mathbf{D_g} - \mathbf{A_d}$.

A. Closed-loop Dynamics

The linear control protocol, (15), along with the description of the communications network can be combined with (12) to obtain the closed-loop equations. To simplify this task, first we solve the integral terms in (15).

$$\int_0^t e_{l,i}(\tau)d\tau = \delta_i - \delta_i^0 = \Delta\delta_i \tag{16}$$

Now, if we replace (16) and (14) into (15), we can have a differential representation of the system that only depends on state variables $\mathbf{\Delta}\delta$ and $\mathbf{\Delta}\omega$.

$$\mathbf{\Delta P_s} = -(k_p\mathbf{I\Delta}\omega + k_i\mathbf{I\Delta}\delta + k_{cp}\mathbf{L\Delta}\omega + k_{ci}\mathbf{L\Delta}\delta) \tag{17}$$

Replacing (17) in (12) we obtain a closed loop system of the form $\dot{\mathbf{x}} = \mathbf{A_c x}$ where $\mathbf{A_c}$ is defined as (18).

$$\mathbf{A_c} = \begin{bmatrix} \mathbf{0} & \mathbf{I} \\ -\mathbf{A_c^{2,1}} & -\mathbf{A_c^{2,2}} \end{bmatrix} \tag{18}$$

$$\mathbf{A_c^{2,1}} = \mathbf{M}^{-1}\left[\mathbf{K_{\Delta\delta}} + \mathbf{K_{P_s}}\left(k_i\mathbf{I} + k_{ci}\mathbf{L}\right)\right] \tag{19}$$

$$\mathbf{A_c^{2,2}} = \mathbf{M}^{-1}\left[\mathbf{D} + \mathbf{K_{P_s}}\left(k_p\mathbf{I} + k_{pi}\mathbf{L}\right)\right] \tag{20}$$

We can verify that, given a choice of $\mathbf{L}$, k_p, k_i, k_{cp} and k_{ci}, the closed-loop system is stable, under the aforementioned assumptions, by calculating the eigenvalues of (18).

IV. Numerical Results

We evaluate the performance of the cooperative controller by carrying out simulations in the IEEE 39-bus test system developed in MATLAB/Simulink [12]. The power system stabilizers implemented in [12] are disabled unless otherwise noted. We consider that the communication links connect each agent to two generators with strong electrical connection (see Fig. 2), as depicted in Fig. 3.

In order to take into account the limited power availability of storage, the maximum power output of each DESS is set to 10% of the power output of the local generator unit ($P_{m,i}$). We assume that enough energy is available for stabilization purposes due to the short time-frame of the simulation. The controller was implemented with a sampling period of $2/60$ s.

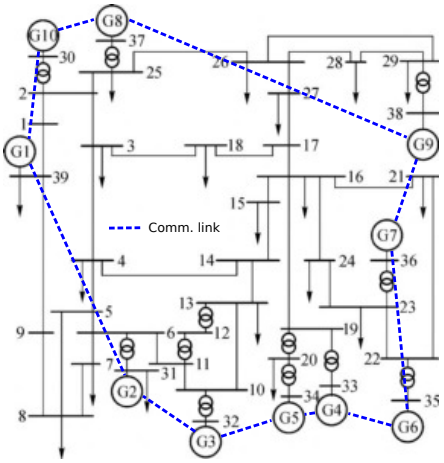

Fig. 3. Structure of the 39 bus tests system and the communication links between agents.

The control gains were selected as $k_p = 100/(2\pi 60)$, $k_i = 3$, $k_{cp} = 30/(2\pi 60)$ and $k_{ci} = 15$. The ability of the controller to guarantee transient stability is tested for a solid three-phase fault applied bus 17 in line 16-17, 0.5 s after the simulation starts. The fault is cleared by opening circuit breakers 100 ms after the fault occurs, unless otherwise stated. The system in open loop is unstable when this fault is applied (see Fig. 6 for eigenvalues of open loop system). When in such conditions, the cooperative control responds as shown in Fig. 4, where we can see the evolution of rotor angles and speeds towards a post-disturbance stable operating point after the second swing. The stabilization time is defined as the time between fault inception and the time when the speed of all generators to is returned to the synchronous frequency of 60 Hz within a tolerance of 0.05 Hz, i.e., the range from 59.95 Hz and 60.05 Hz. These limits are seen as horizontal dashed lines in the rotor speed plot of Fig. 4. This stabilization criterion is inspired by the Frequency Trigger Levels of 0.05 Hz deviation by North American Electric Reliability Corporation [13].

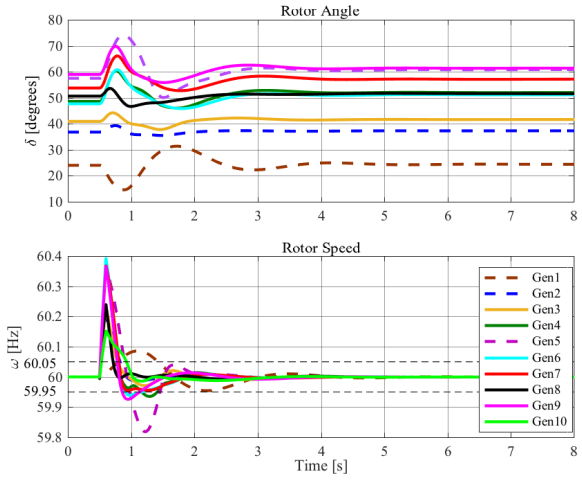

Fig. 4. Plots of generator rotor angles (top) and speeds (bottom) showing the response of the closed-loop system using the proposed cooperative technique.

We compare the performance of our method to a Multi-band Power System Stabilizer (MB-PSS) as implemented in [12] and to the PFL controller [5] with gains $\alpha = 1$

and $\beta = 0$. Since the goal is to verify the ability of the controller to increase the transient stability margins when subject to a fault, we evaluate the capacity of each controller to improve the critical clearing time. That is done by performing multiple simulations for increasing fault clearing times and then obtaining the critical clearing time for each method. Additionally, the ability of the control scheme for stabilizing the system quickly is evaluated, as shown in Fig. 5. The cases when the control scheme failed to stabilize the system were omitted from Fig. 5.

The critical clearing time for MB-PSS was 0.235 s and for PFL, 0.26 s. The proposed distributed method was capable of extending the critical clearing time of the aforementioned decentralized protocols by 35 ms and 10 ms, respectively, achieving 0.27 s. Additionally, the stabilization times obtained by employing the cooperative protocol were smaller in all cases than the MB-PSS and in most cases than PFL. The cooperative controller was especially faster in stabilizing the grid than the PFL in cases where both methods were approaching their limits, when PFL was more than 2 s slower. These results shows that not only our cooperative control can outperform MB-PSS and PFL in terms of critical clearing time but it can also stabilize the system in less time in the same conditions. The mathematical model of the system was evaluated by calculating the eigenvalues of the 39-bus system in open loop and closed loop. The results of the analysis are shown in Fig. 6. While the open loop system is unstable because it eigenvalues with real part equal to zero and multiplicity equal to two or higher, the closed-loop system has only eigenvalues with negative real part and is therefore asymptotically stable.

V. Conclusion

In this paper, we presented a novel cooperative control of DESS capable of coordinating actions of neighboring agents to improve transient stability margins of smart grids. Moreover, linear models that incorporate DESS in its formulation were developed. The performance of the designed controller is numerically validated in MATLAB/Simulink. The simulation results show that by employing fast DESS and inter-agent communication links, the proposed controller can achieve better transient stability performance in terms of critical clearing time than conventional PSS methods and the PFL method. In addition, it was capable of achieving faster stabilization than the PFL when close to the critical clearing time. These results highlight that DESS have the potential to contribute to power grid stability, making it more reliable and secure.

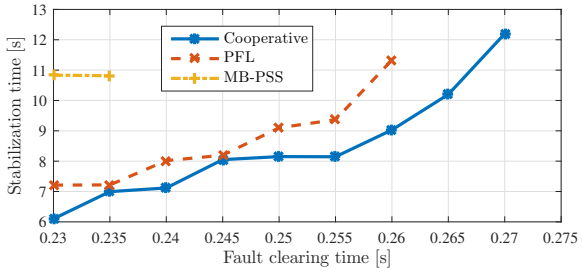

Fig. 5. Comparison of clearing times after a three-phase fault in bus 17 for all three methods.

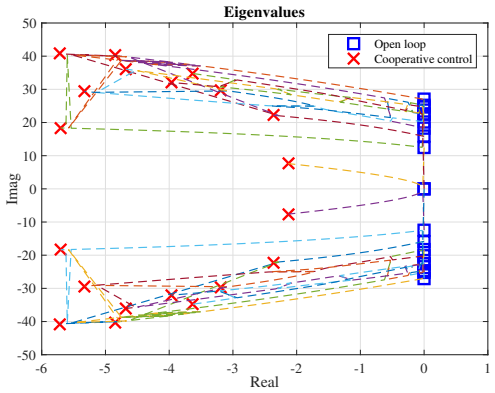

Fig. 6. Eigenvalues of open loop system (blue squares) and closed loop system using the cooperative control (red crosses).

Acknowledgment

The research reported here was partially supported by the National Science Foundation under grant CPS-1646229 and by Nanjing SilverMicro Electronics Ltd.

References

[1] B. J. Kirby, "Frequency regulation basics and trends," United States Department of Energy, Tech. Rep., 2004.

[2] P. D. H. Hines, I. Dobson, and P. Rezaei, "Cascading power outages propagate locally in an influence graph that is not the actual grid topology," *IEEE Transactions on Power Systems*, vol. 32, no. 2, pp. 958–967, March 2017.

[3] M. Andreasson, "Control of multi-agent systems with applications to distributed frequency control power systems," Master's thesis, KTH Royal Institute of Technology, 2013.

[4] J. W. Chapman, M. D. Ilic, C. A. King, L. Eng, and H. Kaufman, "Stabilizing a multimachine power system via decentralized feedback linearizing excitation control," *IEEE Transactions on Power Systems*, vol. 8, no. 3, pp. 830–839, Aug 1993.

[5] A. Farraj, E. Hammad, and D. Kundur, "A cyber-enabled stabilizing control scheme for resilient smart grid systems," *IEEE Trans. Smart Grid*, vol. 7, no. 4, pp. 1856–1865, July 2016.

[6] M. Ayar, R. D. Trevizan, S. Obuz, A. S. Bretas, and H. Latchman, "A robust decentralized control framework for enhancing smart grid transient stability," in *IEEE PES General Meeting*. Chicago, IL: IEEE, July 2017, pp. 1–6.

[7] M. Ayar, S. Obuz, R. D. Trevizan, A. S. Bretas, and H. Latchman, "A distributed control approach for enhancing smart grid transient stability and resilience," *IEEE Transactions on Smart Grid*, vol. 8, no. 6, pp. 3035 – 3044, November 2017.

[8] M. Ayar, R. D. Trevizan, S. Obuz, A. S. Bretas, and H. Latchman, "A cyber-physical robust control framework for enhancing transient stability of smart grids," *IET Cyber-Physical Systems*, vol. 2, no. 4, pp. 198 – 206, December 2017.

[9] P. Kundur, N. J. Balu, and M. G. Lauby, *Power system stability and control*. McGraw-hill New York, 1994, vol. 7.

[10] E. Ghahremani and I. Kamwa, "Online state estimation of a synchronous generator using unscented kalman filter from phasor measurements units," *IEEE Transactions on Energy Conversion*, vol. 26, no. 4, pp. 1099–1108, 2011.

[11] S. H. Horowitz and A. G. Phadke, *Power system relaying*. John Wiley & Sons, 2008, vol. 22.

[12] A. Moeini, I. Kamwa, P. Brunelle, and G. Sybille, "Open data ieee test systems implemented in simpowersystems for education and research in power grid dynamics and control," in *2015 50th UPEC*, 2015, pp. 1–6.

[13] NERC Resources Subcommittee, "Balancing and frequency control," *NERC, Washington, DC, USA, Tech. Rep., Jan*, 2011.